Manipulability analysis to improve the performance of a 7-DoF serial manipulator*

Ali Kanso[1], Marco Schneider[2] and Rainer Müller[2]

***Abstract*— Redundant robots offer significant potential for optimization strategies aimed at enhancing their performance. This paper conducts a kinematic analysis of a 7-DoF manipulator, addressing the inverse kinematic problem and discussing a method for optimizing the robot configuration. Furthermore, the condition number of the Jacobian matrix is introduced as a performance index within the context of this work. Finally, the results are validated through a sensitive robot application, where the accuracy of the estimated force serves as a performance indicator for the manipulator.**

I. INTRODUCTION

Serial industrial robots have mostly six DoF in order to handle parts and performs task in three dimensional space. Robots that have more DoF than the minimum number required to perform a defined tasks are classified as "redundant" robots [1]. Redundancy can be applied to solve various tasks in robotics, such as avoiding singularity and collisions, improving mechanical advantage, manipulability, and performance [1].

Manipulators with seven DoF have mostly an infinite number of possible joint configuration to solve the inverse kinematic problem. Solving the aforementioned problem is a hard task and depend on the kinematic chain of the manipulator. Solving the inverse kinematic problem is essential for implementing optimization methods on redundant robots. Several researchers developed and proposed different optimization strategies for redundant robots [2]. Within this scope, measuring the manipulability is well-know technique to evaluate the performance of a manipulator. Yoshikawa [3] introduced the manipulability index to examine how suitable an adaption of the workspace is possible [4]. Salisbury and Craig [5] introduced the Jacobian matrix's condition number as a performance index to assess the performance characteristics of robot manipulators, as discussed by Tanev [6]. In this paper, a method for solving the inverse kinematics of a redundant 7-DoF robot (KUKA LBR iiwa) on the basis of a closed-form solution is presented. In addition, a method for optimizing the robot configuration using the Jacobian matrix condition number as a performance index is discussed. The accuracy of force estimation on the robot flange in cartesian space, based on measuring joint torques and performing a force-controlled application was used as a measure for robot performance.

*The results are part of the project "Entwicklung eines Versuchswicklers", funded by the central innovation program in Saarland. Furthermore the research is funded by the Interreg V A Großregion within Robotix-Academy project (no 002-4-09-001).

[1]: Professor of robotics at the Technische Hochschule Ingolstadt (THI), Ingolstadt, 85049, Germany ali.kanso@thi.de

[2]: Chair of Assembly Systems at the Center Mechatronics and Automation Technologies, Saarbrücken, 66121, Germany {m.schneider, rainer.mueller}@zema.de

II. ANALYSIS OF THE ROBOT KINEMATICS

A. Symbolic notation for kinematic modeling

Serial robots have open kinematic structures that allow their kinematics to be modeled using simple mathematical approaches. The position and orientation of each link of the robot can be represented by a link-fixed coordinate system (*CS*). The geometric relationship between two coordinate systems in 3D space is typically described by six parameters, three of them are essential for the position and three for the orientation.

Richard S. Hartenberg, an American engineer and former VDI member, and the French engineer Jacques Denavit introduced a convention for modeling serial robots with only four parameters ($\delta_{i,i-1}(z_{i-1})$, $d_{i,i-1}(z_{i-1})$, $l_{i,i-1}(x_i)$ and $\alpha_{i,i-1}(x_i)$) per joint transition [7]. These parameters represent a rotation and translation around the z_{i-1}-axis and rotation and translation about the x_i-axis, respectively.

The reason for having only four DH parameters lies in the convention used to define the link-fixed coordinate systems. Despite the widespread use of Denavit's and Hartenberg's convention, it does not have a common name in the literature. It is commonly known as the Denavit-Hartenberg convention, DH convention or classical DH convention. In 1956, it was introduced in a VDI report as the HD convention (see [8], [9], [10]). The term DH convention is used in this article.

The DH transformation of two consecutive coordinate systems (CS_{i-1} and CS_i) can be calculated by multiplying the following individual transformation matrices:

$$^{i-1}\mathbf{T}_i = Rotation(\delta_{i,i-1}, z_{i-1}) \cdot Translation(d_{i,i-1}, z_{i-1}) \cdot Translation(l_{i,i-1}, x_i) \cdot Rotation(\alpha_{i,i-1}, x_i) \quad (1)$$

The DH parameters of the model are integrated into the robot controller so that it can perform basic kinematic tasks such as solving direct and inverse kinematic problems. Consequently, the controller can master the robot motion and monitor the position of the end effector.

Manuscript 338 submitted to 2024 10th International Conference on Control, Decision and Information Technologies (CoDIT). Received March 4, 2024.

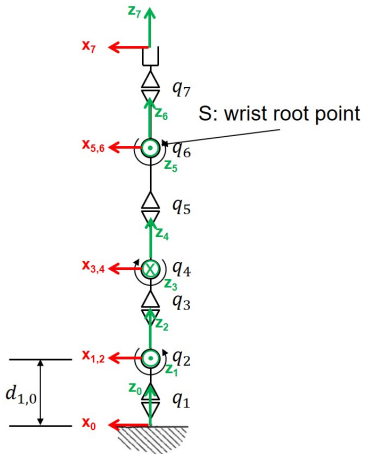

Fig. 1. Kinematic modeling of the KUKA LBR iiwa [11]

As outlined in Kanso's dissertation [11], the KUKA LBR iiwa robot is considered and modeled using the DH convention. To enhance the reader's comprehension within the context of this paper, we present and discuss the modeling of the KUKA LBR iiwa (see fig. 1).

The corresponding DH parameters are listed in table I.

Link i	1	2	3	4	5	6	7
$\delta_{i,i-1}[^\circ]$	q_1	q_2	q_3	q_4	q_5	q_6	q_7
$d_{i,i-1}[m]$	0,36	0	0,42	0	0,4	0	0,126
$l_{i,i-1}[m]$	0	0	0	0	0	0	0
$\alpha_{i,i-1}[^\circ]$	$-\frac{\pi}{2}$	$\frac{\pi}{2}$	$\frac{\pi}{2}$	$-\frac{\pi}{2}$	$-\frac{\pi}{2}$	$\frac{\pi}{2}$	0

TABLE I
DH PARAMETERS OF THE KUKA LBR IIWA [11]

B. Inverse kinematic problem

Several authors [12][13][14][15][16][17][18] have been exploring analytical approaches to solving the inverse kinematic problem of a 7-DoF robot for several years. Most of these approaches involve decomposing the robot's kinematics into two parts and fixing one joint angle while varying all other angles to determine multiple solutions for the inverse kinematics of a predefined robot pose.

In his dissertation, Kanso [11] investigated a simple analytical approach to solve the inverse kinematic problem for a 7-DoF robot, in particular the KUKA LBR iiwa. In order to simplify and supplement the content of this paper the approach is explained and discussed below.

As previously stated, the inverse kinematic problem involves determining the joint variables based on a given pose ${}^{base}\underline{w}_{TCP}$ of a specified TCP (Tool-CenterPoint) in cartesian space. In the initial stage, the problem is simplified to the inverse kinematic problem of a 6-DoF robot. Consequently, the redundant joint is constrained, and its angle $\delta_{3,2}$ is fixed at zero. In order to achieve zero-space motion by altering the kinematic configuration of the robot while maintaining the pose of the TCP, the redundant angle $\delta_{3,2}$ must be interpolated while keeping the joint $\delta_{4,3}$ fixed at the value determined in the initial step when the redundant angle $\delta_{3,2}$ was set to zero. The wrist root point S is defined as the intersection point of the last three axes (see Fig. 1). The origin of coordinate system CS_5 is attached to point S. Therefore, the mathematical description of a coordinate system attached to point S in relation to the robot base coordinate system can be calculated as follows:

$$
\begin{aligned}
{}^{Base}\mathbf{T}_S &= {}^{Base}\mathbf{T}_1 \cdot {}^{1}\mathbf{T}_2 \cdot {}^{2}\mathbf{T}_3 \cdot {}^{3}\mathbf{T}_4 \cdot {}^{4}\mathbf{T}_5 \\
&= \begin{pmatrix} {}^{Base}\mathbf{D}_S & \begin{matrix} c_1 \cdot s_2 \cdot d_{3,2} + d_{5,4} \cdot (c_1 \cdot c_4 \cdot s_2 - s_4 \cdot (c_1 \cdot c_2 \cdot c_3 - s_1 \cdot s_3)) \\ s_1 \cdot s_2 \cdot d_{3,2} + d_{5,4} \cdot (s_1 \cdot s_2 \cdot c_4 - s_4 \cdot (c_1 \cdot s_3 + c_2 \cdot c_3 \cdot s_1)) \\ c_2 \cdot d_{3,2} + d_{1,0} + d_{5,4} \cdot (c_2 \cdot c_4 + s_2 \cdot s_4 \cdot c_3)) \end{matrix} \\ \underline{0}^T & 1 \end{pmatrix}
\end{aligned} \tag{2}
$$

Where $s_i = sin(\delta_{i,i-1})$ and $c_i = cos(\delta_{i,i-1})$.

The vector composed of the first three elements in the fourth column of the matrix in equation 2 indicates the position of the wrist root point S in relation to the robot's base coordinate system ${}^{Base}\underline{r}_S$. The latter depends on the values of the first, second, third, and fourth joint angles, given that the third and fourth rotation angles are already known. Consequently, the values of the first two rotation angles can be determined. Furthermore, the transformation matrix ${}^{Base}\mathbf{T}_S$ and thereby the position vector ${}^{Base}\underline{r}_S$ can be determined by following these steps:

$$
{}^{Base}\mathbf{T}_S = {}^{Base}\mathbf{T}_{TCP} \cdot {}^{S}\mathbf{T}_{TCP}^{-1} \tag{3}
$$

$$
\rightarrow {}^{Base}\mathbf{T}_S = \begin{pmatrix} {}^{Base}\mathbf{D}_S & \begin{matrix} {}^{Base}x_S \\ {}^{Base}y_S \\ {}^{Base}z_S \end{matrix} \\ \underline{0}^T & 1 \end{pmatrix} \tag{4}
$$

Comparing the translational components of the matrices in equations 2 and 4 results in the following system of equations:

$$
a_x(s_2, c_2) \cdot c_1 + b_x \cdot s_1 = {}^{Base}x_S \tag{5}
$$

$$
a_y \cdot c_1 + b_y(s_2, c_2) \cdot s_1 = {}^{Base}y_S \tag{6}
$$

$$
a_z \cdot c_2 + b_z \cdot s_2 = {}^{Base}z_S - d_{1,0} \tag{7}
$$

The equation 7 is to be solved similarly to the equation $a \cdot cos(\theta) + b \cdot sin(\theta) = c$, where a, b and c are constants and θ is the angle to be determined. A solution to this equation is outlined in [11], yielding two solutions for $\delta_{2,1}$.

$$
\delta_{2,1_1} = arctan2\left(\frac{2 \cdot t_{\delta_{2,1_1}}}{1 + t^2_{\delta_{2,1_1}}}, \frac{1 - t^2_{\delta_{2,1_1}}}{1 + t^2_{\delta_{2,1_1}}}\right) \tag{8}
$$

$$
\delta_{2,1_2} = arctan2\left(\frac{2 \cdot t_{\delta_{2,1_2}}}{1 + t^2_{\delta_{2,1_1}}}, \frac{1 - t^2_{\delta_{2,1_2}}}{1 + t^2_{\delta_{2,1_2}}}\right) \tag{9}
$$

Manuscript 338 submitted to 2024 10th International Conference on Control, Decision and Information Technologies (CoDIT). Received March 4, 2024.

Here $t_{\delta_{2,1_1}}$ and $t_{\delta_{2,1_2}}$ are defined as follows:

$$t_{\delta_{2,1_1}} = \frac{b_z}{a_z + ({}^{Base}z_S - d_{1,0})} + \frac{\sqrt{a_z^2 + b_z^2 - ({}^{Base}z_S - d_{1,0})^2}}{a_z + ({}^{Base}z_S - d_{1,0})} \tag{10}$$

$$t_{\delta_{2,1_2}} = \frac{b_z}{a_z + ({}^{Base}z_S - d_{1,0})} - \frac{\sqrt{a_z^2 + b_z^2 - ({}^{Base}z_S - d_{1,0})^2}}{a_z + ({}^{Base}z_S - d_{1,0})} \tag{11}$$

Hence s_2 and c_2 can be calculated and subsequently substituted into $a_x(s_2, c_2)$ and $b_y(s_2, c_2)$ (see eqs. 5 and 6), respectively. Consequently, s_1 and c_1 can be determined from the system of equations of eq. 5 and 6 can be calculated as follows:

$$s_1 = \frac{a_y \cdot c_x - a_x \cdot c_y}{a_y \cdot b_x - a_x \cdot b_y};\ c_1 = \frac{b_y \cdot c_x - b_x \cdot c_y}{b_y \cdot a_x - b_x \cdot y_y} \tag{12}$$

The angle of rotation $\delta_{1,0}$ can then be determined as follows:

$$\delta_{1,0} = arctan2(s_1, c_2) \tag{13}$$

Thus, for $\delta_{1,0}$ there are two solutions depending on the joint angle $\delta_{2,1}$.

The last three joint angles ($\delta_{4,5}, \delta_{5,6}$ and $\delta_{6,7}$) can be determined, as elucidated in [11], through a comparison with a suitable Euler angle convention (ZY'Z").

III. FORCE ESTIMATION AND MANIPULABILITY OF A SERIAL ROBOT

External forces can have various impacts throughout the planning and execution of compliant robot motions [19]. Therefore, the accuracy of force determination significantly influences the performance of a robot, particularly in compliant robot behavior and force-controlled robot applications. There are different concepts employed by robot manufacturers for estimating external force/torque in serial robot kinematics. Universal Robots integrates a 6-DoF force/torque sensor into the last link of its e-series robots [20]. In contrast, Fanuc integrates the force/torque sensor into the base of its CR series [21] robot family. Additionally, the KUKA LBR iiwa [22] and KUKA LBR 4+ are equipped with a 1-DoF torque sensor on each joint to estimate the joint torque.

The KUKA LBR iiwa robot has integrated torque sensors in each joint. Therefore, the joint torques $\underline{\tau}$ are measured directly by the integrated sensors. The force/torque vector $\underline{K}$, representing the force and torque exerted on the end effector and expressed in the TCP-*CS*, is then determined as described in eq. 14. The calculation relies on the measured joint torques $\underline{\tau}$ and the kinematic configuration of the robot, which is represented by the inverse of the geometric Jacobian matrix $\mathbf{J}_g$ [11].

$$\underline{K} = \mathbf{J}_g^{-T} \cdot \underline{\tau} \tag{14}$$

The external torques $\underline{\tau}_e$ are then calculated by subtracting the gravitational torques from the measured joint torques [23]. The accuracy of the estimation of the gravitational torques depends on the dynamic and kinematic model of the robot as well as on the accuracy of the model parameters for the tools and elements mounted on the robot. The relevant external force/toque $\underline{K}_e$ (see eq. 15) is then determined analogously to eq. 14, based on the external torques $\underline{\tau}_e$ and inverse of the geometric Jacobian matrix $\mathbf{J}_g$ [11].

$$\underline{K}_e = \mathbf{J}_g^{-T} \cdot \underline{\tau}_e \tag{15}$$

From the eqs. 14 and 15 it can be concluded that the accuracy of the force/torque estimation in cartesian space is not only dependent on the accuracy of the measured joint torques, but also on the invertibility of the geometric Jacobian matrix $\mathbf{J}_g$. The inverse of the Jacobian matrix cannot be computed using classical methods when the matrix is singular. In such cases, the pseudo-inverse of the matrix can be determined, for example, using the Singular Value Decomposition (SVD) algorithm. However, even in such cases, it still does not yield a more accurate inverse of the Jacobian matrix when it is singular. In such situations, the robot is situated within a singularity, where it effectively loses one or more degrees of freedom. Therefore, certain tasks may not be achievable in this case. Additionally, near a singularity, the robot exhibits low performance, and its actions may be poorly conditioned. The accuracy of force estimation mentioned above (eqs. 14 and 15) will be negatively affected near singularities, as the inversion of the Jacobian matrix is not accurate in such cases.

Several indices have been proposed to quantify the invertibility of the Jacobian matrix. The analysis and optimization of such indices during the design and development period could lead to a robot design with a maximally large, well-conditioned workspace [24]. The determinant of the Jacobian matrix is proposed as an index for quantifying the manipulability of the kinematics and can also be determined as follows in the case of a non-square matrix:

$$\kappa = \sqrt{det(\mathbf{J}_g \cdot \mathbf{J}_g^T)} = |det(\mathbf{J}_g)| \tag{16}$$

In this context, singular configurations are defined when the determinant of the Jacobian matrix is zero. Moreover, a well-designed robot implies that large regions of its workspace are characterized by high values of κ.

Indices proposed for quantifying the manipulability of a serial robot can be found in [25][24]. A method relying on calculation the condition number of the geometric Jacobian matrix $\mathbf{J}_g$ was presented in [26].

$$c(\mathbf{J}_g) = ||\mathbf{J}_g|| \cdot ||\mathbf{J}_g^{-1}|| \tag{17}$$

Where $||\mathbf{J}_g||$ is the norm of the Jacobian matrix. Moreover, the literature provides various approaches to calculate matrix norms. Consequently, the condition number is influenced by the selection of the matrix norm. The 2-norm and the Frobenius norm are among the most commonly used matrix

norms [27]. The 2-norm is defined as the square root of the largest eigenvalue of the matrix $\mathbf{J}_g \cdot \mathbf{J}_g^T$. The condition number of the Jacobian matrix $\mathbf{J}_g$ is defined as the ratio between the largest λ_{max} and the smallest λ_{min} eigenvalue of the matrix $\mathbf{J}_g \cdot \mathbf{J}_g^T$. Thus, the condition number can be calculated as follows:

$$c(\mathbf{J}_g) = \sqrt{\frac{\lambda_{max}}{\lambda_{min}}} = \frac{\sigma_{max}}{\sigma_{min}} \tag{18}$$

Where the parameters σ_{max} and σ_{min} are respectively the largest and smallest singular values of the matrix $\mathbf{J}_g \cdot \mathbf{J}_g^T$. Eq. 18 is utilized to calculate the condition number as an index for quantifying the manipulability of the robot in the context of this paper.

Based on the eq. 18, the smallest possible value of the condition number is equal to 1. In this scenario, the matrix is isotropic and the robot is then considered to have isotropic behavior [28]. Errors in the joint torques are therefore mapped one-to-one to the force/torque vector in cartesian space. In this context, the condition number can be interpreted as a measure of the accuracy with which the mechanism generates the targeted output forces and torques at the end effector from the input torques of the joints [29][25]. To enhance the accuracy of the estimated force/torque vector in cartesian space, kinematic configurations of the robot with a low condition number, ideally close to one, should be identified and applied.

IV. Optimization of the Configuration of a 7-DoF Manipulator

In [11], an approach for optimizing the robot configuration of a 7-DoF robot in the static state for a predefined pose was presented. However, as the typical task in the industrial environment involves executing a predefined trajectory rather than just a predetermined pose, the approach presented in [11] was expanded within the framework of this work. Thus, an optimization method is developed to identify the optimal robot configuration, enhancing the robot's performance along a trajectory.

As described above, a 7-DoF robot offers the possibility to perform a zero-space motion due to its additional degree of freedom, i.e. to adapt its configuration by utilizing the redundancy angle $\delta_{3,2}$ while maintaining at the same pose. During a so-called Continuous Path (CP) movement, the KUKA LBR iiwa keeps its redundancy angle constant.

The aim of the optimization is to minimize inaccuracies in the force estimation by ensuring that the condition number of the Jacobian matrix remains as low as possible during a trajectory. Ideally, it should be one in the best case.

IIn the first step, the predefined trajectory is discretized into finite discrete poses in the simulation environment, which is set up by means of Matlab. There are eight solutions for the inverse kinematic problem for a constant redundancy angle. In the second step, the redundancy angle is interpolated along its range (axis range between -170° and 170°), and the inverse kinematic problem is solved for every interpolated angle, as mentioned in Section II-B. This results in a finite number of inverse kinematic solutions based on the interpolation resolution of the redundancy angle. The condition number is then calculated for every possible solution of the inverse kinematics for each discretized pose. The calculated condition number is then stored in a three-dimensional matrix (see Fig. 2).

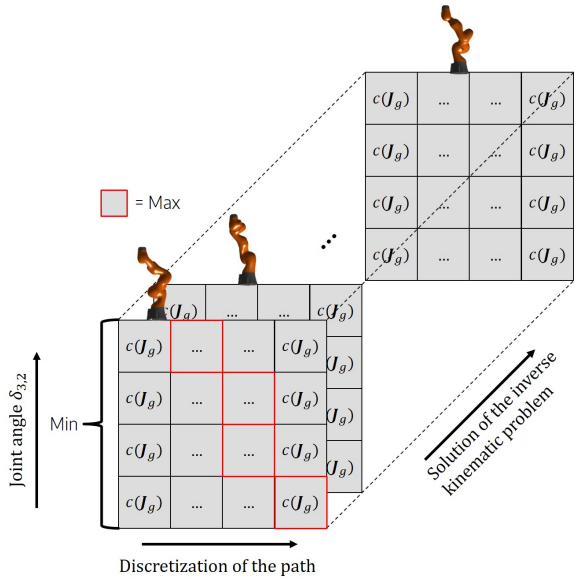

Fig. 2. Scheme of the optimization strategy

Each row of the three-dimensional matrix represents the discretized trajectory. The maximum condition number of the Jacobian matrix is determined for each interpolated configuration along the discretized trajectory. This particular configuration denotes the discretized pose characterized by the poorest kinematic manipulability within the robot's kinematics for the relevant configuration along the discretized trajectory. On the basis of the maximum condition number of every interpolated configuration the individual trajectories can be compared with each other. Since the lowest possible condition number promises a high accuracy of force and torque determination, the minimum of all maxima is determined. This ensures that for this trajectory the condition number of the Jacobian matrix does not exceed the value of the determined minimum. As a result, the best configuration for the robot manipulability is identified.

For a better understanding, the three-dimensional matrix is shown as a surface plot in Fig. 3. Obviously, the condition number of the Jacobian matrix changes along the trajectory, and the redundancy angle $\delta_{3,2}$ impacts both the condition number of the Jacobian matrix and, consequently, the manipulability of the robot.

Manuscript 338 submitted to 2024 10th International Conference on Control, Decision and Information Technologies (CoDIT). Received March 4, 2024.

Furthermore, although there are eight inverse kinematics solutions for a fixed redundancy angle, the kinematic structure of the robot leads to the formation of only two distinct groups of robot configurations. This distinction is made by comparing their respective condition numbers. Thus, the described optimization process theoretically provides four equivalent solutions, representing the same trajectory and the same course of the condition number, enabling the precise determination of forces and torques.

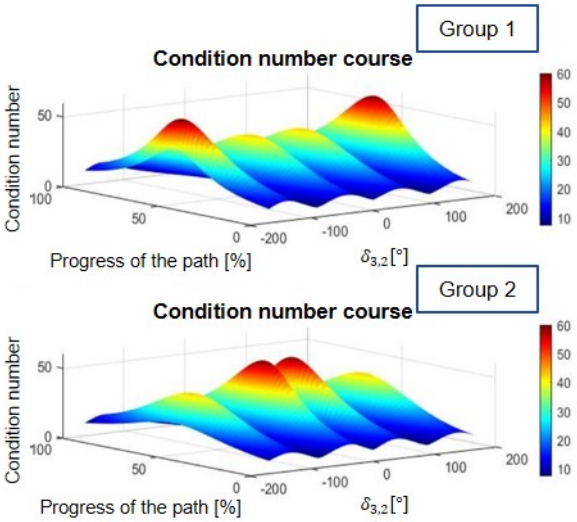

Fig. 3. Surface plot of the condition number along a predefined trajectory

V. IMPLEMENTATION AND VALIDATION

Initially, an experiment was conducted to illustrate how the invertibility and conditioning of the Jacobian matrix impact the accuracy of mapping joint torques to cartesian forces/torques at the robot flange, as discussed in Section III.

Therefore, the KUKA LBR iiwa executed a force controlled motion along a defined path and applied a constant force. The robot was programmed to move from point A to point B while applying a force of 40 N in the negative z-direction of the wave block-CS $\left({}^{WB}\underline{z}\right)$ (see Fig. 5).

Fig. 4 shows a graphical visualization of the condition number of the Jacobian matrix along the trajectory calculated according to equation 18 together with the corresponding force estimation of the robot. This shows that the condition number plot and the force plot reach their peaks at the same position. Thus, the inaccuracy of the estimated force are caused by the poor conditioning of the robot configuration.

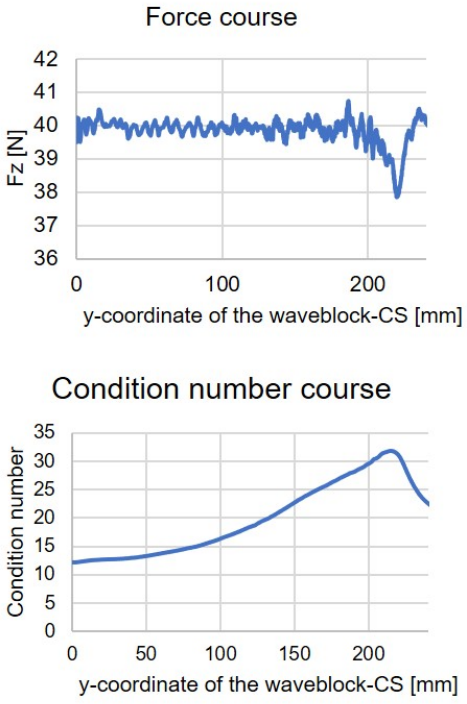

Fig. 4. Condition number progression along a robot path

In order to validate the optimization approach from section IV, the described force-controlled motion was performed again after the optimization. The redundancy angle $\delta_{3,2}$ and thus the configuration of the robot was adapted so that the path has the lowest possible condition number of the Jacobian matrix. Fig. 5 illustrates the relationship between the condition number of the Jacobian matrix and the ability to apply a constant force while moving after optimizing the robot configuration.

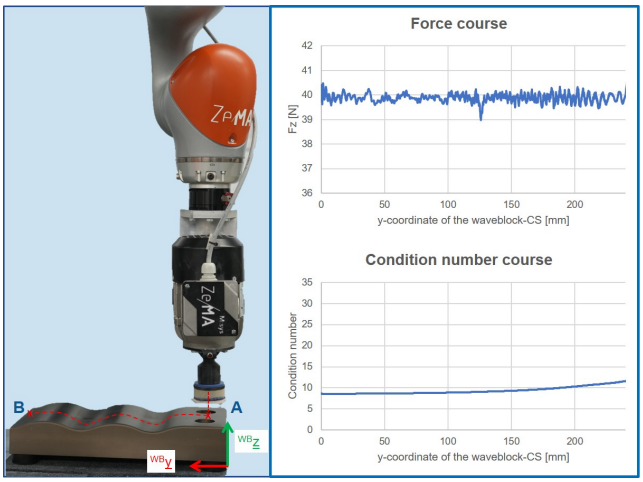

Fig. 5. Example of a force-controlled motion on a wave block with different configurations

It can be clearly seen that the poorly conditioned configuration from Fig. 4 results in inaccurate force estimation. The inaccuracy at the peak is about 2 N. In comparison to

that the good configuration from Fig. 5 provides a stable and accurate force curve due to the optimized kinematic configuration. Thus, the developed optimization strategy can be applied to improve the manipulability of the robot as well as the accuracy of force estimation and the performance of implementing force-controlled tasks.

VI. CONCLUSION

The performance of sensitive and redundant robot systems is crucial for their deployment in assembly and manufacturing technologies. This paper presents a closed-form solution for the inverse kinematic problem of a 7-DoF robot as well as a kinematic optimization strategy for the robot configuration.

The condition number of the Jacobian matrix serves as a performance index within the developed optimization strategy. The accuracy of force estimation is enhanced, enabling the execution of force-controlled applications with greater precision. This improvement is particularly crucial for robotic applications such as AI-based sensitive assembly tasks (e.g., Peg in Hole) [30], where the success of the assembly relies directly on the force and torque data of the robot. Additionally, in robotic sanding applications, maintaining a constant contact force is a decisive factor for task execution [31].

Further studies will investigate the adaptability of the presented optimization strategy to solve other problems, e.g. energy-efficient path planning and work space analysis.

REFERENCES

[1] K. Kreutz-Delgado, M. Long, and H. Seraji. Kinematic analysis of 7 dof anthropomorphic arms. In *IEEE International Conference on Robotics and Automation*, pages 824–830 vol.2, 1990.

[2] S. Yuan, H. Zhang, N. Wang, and N. Luan. Motion study of a redundant 7-dof operation robot. In *2011 international conference on electrical and control engineering*, pages 3056–3060. IEEE, 2011.

[3] T. Yoshikawa. Manipulability of robotic mechanisms. *The International Journal of Robotics Research*, 4(2):3–9, 1985.

[4] N. Vahrenkamp, T. Asfour, G. Metta, G. Sandini, and R. Dillmann. Manipulability analysis. In *2012 12th IEEE-RAS International Conference on Humanoid Robots (Humanoids 2012)*, pages 568–573, 2012.

[5] J. K. Salisbury and J. J. Craig. Articulated hands: Force control and kinematic issues. *The International Journal of Robotics Research*, 1(1):4–17, 1982.

[6] T. Tanev and B. Stoyanov. On the performance indexes for robot manipulators. *Problems of engineering cybernetics and robotics*, 49:64–71, 2000.

[7] R. S. Hartenberg and J. Denavit. *A kinematic notation for lower pair mechanisms based on matrices*. *Journal of applied mechanics*, 77(2):215–221, 1955.

[8] R. Müller. *Verbesserung des kinematischen und dynamischen Bewegungsverhaltens von Handhabungsgeräten mit geschlossenen kinematischen Teilketten: Parameteridentifikation, Bahnplanung und Bahnoptimierung, Verformungskompensation*. PhD thesis, RWTH (Rheinisch-Westflische Technische Hochschule) Aachen, 1996.

[9] M. Weck. *Werkzeugmaschinen Fertigungssysteme: Automatisierung von Maschinen und Anlagen*. VDI-Buch. Springer-Verlag Berlin Heidelberg, 5., neu bearbeitete auflage edition, 2001.

[10] H. Kerle, B. Corves, and M. Hüsing. *Getriebetechnik: Grundlagen, Entwicklung und Anwendung ungleichmäßig übersetzender Getriebe*. Studium. Vieweg+Teubner Verlag Wiesbaden, 4., bearbeitete und ergänzte auflage edition, 2011.

[11] A. Kanso. *Konzeption und Realisierung einer sensitiven Montageaufgabe basierend auf einem Handhabungsgerät und intelligenter Sensorik für den Wickelprozess endloser Gummidichtungen*. PhD thesis, University of Saarand and ZeMA gGmbH, 2021.

[12] P. Dahm and F. Joublin. *Closed form solution for the inverse kinematics of a redundant robot arm*. Internal report. Ruhr-Univ., Inst. für Neuroinformatik, 1997.

[13] D. Tolani, A. Goswami, and N. I. Badler. Real-time inverse kinematics techniques for anthropomorphic limbs. *Graphical Models*, 62(5):353–388, 2000.

[14] H. Moradi and S. Lee. Joint limit analysis and elbow movement minimization for redundant manipulators using closed form method. In *Proceedings of the 2005 International Conference on Advances in Intelligent Computing - Volume Part II*, ICIC'05, page 423–432, Berlin, Heidelberg, 2005. Springer-Verlag.

[15] M. Shimizu, H. Kakuya, W.-K. Yoon, K. Kitagaki, and K. Kosuge. Analytical inverse kinematic computation for 7-dof redundant manipulators with joint limits and its application to redundancy resolution. *IEEE Transactions on Robotics*, 24(5):1131–1142, 2008.

[16] Y. Wang and P. Artemiadis. Closed-form inverse kinematic solution for anthropomorphic motion in redundant robot arms. *Advances in Robotics & Automation*, 02, 2013.

[17] D. Zhou, L. Ji, Q. Zhang, and X. Wei. Practical analytical inverse kinematic approach for 7-dof space manipulators with joint and attitude limits. *Intelligent Service Robotics*, 8:215–224, 2015.

[18] D. Busson, R. Bearee, and A. Olabi. Task-oriented rigidity optimization for 7 dof redundant manipulators. *IFAC-PapersOnLine*, 50(1):14588–14593, 2017. 20th IFAC World Congress.

[19] A. Colomé, D. Pardo, G. Alenyà, and C. Torras. External force estimation during compliant robot manipulation. In *2013 IEEE International Conference on Robotics and Automation*, pages 3535–3540, 2013.

[20] Universal Robots. *Cobots from Universal Robots*. https://www.universal-robots.com/products/ur10-robot/, last checked 19.02.2024.

[21] FANUC. *Collaborative Robots of FANUC*. https://www.fanuc.eu/de/en/robots/robot-filter-page/collaborative-robots, last checked 19.02.2024.

[22] KUKA AG. *KUKA LBR iiwa*. https://www.kuka.com/en-de/products/robot-systems/industrial-robots/lbr-iiwa, last checked 19.02.2024.

[23] A. Winkler and J. Suchý. Force-guided motions of a 6-d.o.f. industrial robot with a joint space approach. *Advanced Robotics*, 20(9):1067–1084, 2006.

[24] J. J. Craig. *Introduction to robotics: Mechanics and control. Pearson/Prentice Hall. ISBN:0201543613*, 2005.

[25] A. Sanagoo. *Eine neuartige Roboterkinematik für die laparoskopische Single-Port Chirurgie*. PhD thesis, Fraunhofer-Verlag, 2015.

[26] J. K. Salisbury and J. J. Craig. Articulated hands: Force control and kinematic issues. *The International Journal of Robotics Research*, 1(1):4–17, 1982.

[27] J. P. Merlet. Jacobian, manipulability, condition number and accuracy of parallel robots. In S. Thrun, R. Brooks, and H. Durrant-Whyte, editors, *Robotics Research*, pages 175–184, Berlin, Heidelberg, 2007. Springer Berlin Heidelberg.

[28] F. Ranjbaran, J. Angeles, and A. Kecskemethy. On the kinematic conditioning of robotic manipulators. In *Proceedings of IEEE International Conference on Robotics and Automation*, volume 4, pages 3167–3172 vol.4, 1996.

[29] F. C. Park and R. W. Brockett. Kinematic dexterity of robotic mechanisms. *The International Journal of Robotics Research*, 13(1):1–15, 1994.

[30] N Afifi, M. Schneider, A. Kanso, and R. Müller. High precision peg-in-hole assembly approach based on sensitive robotics and deep recurrent q-learning. In Thorsten Schüppstuhl, Kirsten Tracht, and Jürgen Fleischer, editors, *Annals of Scientific Society for Assembly, Handling and Industrial Robotics 2022*, pages 3–13, Cham, 2023. Springer International Publishing.

[31] M. Schneider, A. Bashir, and R. Müller. Einsatz eines senstiven roboters zur kraftgeregelten bearbeitung von freiform-oberflächen in der keramikindustrie. In Burkhard Corves and Mathias Hüsing, editors, *15. Kolloquium Getriebetechnik*, pages 109–122, 2023.